Supporting Informations for

A pellet-type optical nanomaterial of silica-based naphthalimide-DPA-Cu(II) complexes: recyclable fluorescence detection of yrophosphate with high sensitivity

Jun Feng Zhang,[a,b,§] Minsung Park,[c,§] Wen Xiu Ren,[a] Youngmee Kim,[d] Sung Jin Kim,[d] Jong Hwa Jung*[c] *and* Jong Seung Kim*[a]

[a]*Department of Chemistry, Korea University, Seoul 136-701, Korea.*
[b]*College of Chemistry and Chemical Engineering, Yunnan Normal University, Kunming 650092, P.R. China.*
[c]*Department of Chemistry and Research Institute of Natural Science, Gyeongsang National University, Jinju 660-701, Korea.*
[d]*Department of Chemistry and Nano Science, Ewha Womans University, Seoul 120-750, Korea.*
[§]*Both authors contributed equally to this work.*
**Corresponding authors: E-mail: jonghwa@gnu.ac.kr (J. H. Jung); jongskim@korea.ac.kr (J. S. Kim)*

Materials and Instruments. Unless otherwise noted, materials were obtained from commercial suppliers and were used without further purification. Flash chromatography was carried out on silica gel (230–400 mesh). ^{1}H and ^{13}C NMR spectra were recorded on a Bruker 300 apparatus. Infrared spectra of silica powder pellets were obtained using a Shimadzu FT-IR 8400S and the mass spectrum was obtained with a JEOL JMS-700 mass spectrometer. Transmission electron microscopy (TEM) images were captured with a JEOL JEM−2100 F microscope. Nitrogen-adsorption isotherms were measured at 78 K on a Micromeritics ASAP 2010 analyzer. Thermal gravimetric analysis was conducted on a TA SDT Q600 at a heating rate of 10 °C/min using a Pt pan in air. The temperature was scanned from 25 °C to 900 °C.

For **MSIND**-Cu^{2+}, fluorescence emission spectra were recorded with a Shimadzu RF-5301-PC instrument. Stock solutions (0.01 M) of guest molecules were prepared in H_2O at pH 7. Dispersion of **MSIND-**Cu^{2+} (ligand **1** attached mesoporous silica, 10 μM) was prepared in H_2O. For all measurements, excitation was at 380 nm, with excitation and emission slit widths of 1.5 nm. The pH value was adjusted by using in HEPES buffer solution (0.02 M, pH = 7.4).

Preparation of 3. Under nitrogen, a solution of 4-bromo-1,8-naphthalic anhydride **4** (0.6 g, 2.18 mmol) and di-(2-picolyl)amine (DPA) (0.6 g, 3.02 mmol) in 2-methoxyethanol (50

mL) was refluxed for 48 h, the mixture was evaporated by rotary evaporation and dissolved in CH_2Cl_2 (150 mL). The organic layer was washed with water (3 × 100 mL), dried over anhydrous Na_2SO_4, and filtered. After the solution was evaporated under reduced pressure, the crude product was purified by column chromatography (silica, ethyl acetate/MC 2 : 1) to give 0.68 g of **1** (78% yield). ^{1}H NMR (300 MHz, $CDCl_3$, δ): 8.95 (d, 1H, J = 8.5 Hz), 8.52 (dd, 2H, J = 6.6 Hz), 8.48 (d, 1H, J = 7.3 Hz), 8.26 (d, 1H, J = 8.3 Hz), 7.64 (dd, 1H, J = 7.3 Hz), 7.56 (t, 2H, J = 7.6 Hz), 7.31 (d, 2H, J = 7.8 Hz), 7.17 (d, 1H, J = 8.3 Hz), 7.15–7.11 (m, 2H), 4.72 (s, 4H). ^{13}C NMR (100 MHz, $CDCl_3$, δ): 156.8, 155.2, 149.7, 136.8, 134.4, 133.2, 132.1, 126.4, 126.0, 122.7, 122.4, 119.5, 117.3, 111.4, 59.6. MS (FAB): $[M+H]^+$ calcd for $C_{24}H_{18}N_3O_3$, 396.13; found 396.15.

Preparation of 1. Under nitrogen, a solution of **3** (0.3 g, 0.76 mmol) and *n*-butylamine (0.1 g, 1.37 mmol) in EtOH (50 mL) was refluxed for 24 h, the mixture was evaporated by rotary evaporation and dissolved in CH_2Cl_2 (100 mL). The organic layer was washed with water (3 × 50 mL), dried over anhydrous Na_2SO_4, and filtered. After the solution was evaporated under reduced pressure, the crude product was purified by column chromatography (silica, MC/EtOH 20 : 1) to give 0.29 g of **1** (86% yield). ^{1}H NMR (300 MHz, $CDCl_3$, δ): 8.88 (d, 1H, J = 8.5 Hz), 8.61–8.56 (m, 3H), 8.35 (d, 1H, J = 8.2 Hz), 7.71 (t, 1H, J = 8.5 Hz), 7.58 (t, 2H, J = 7.6 Hz), 7.35 (d, 2H, J = 7.8 Hz), 7.21–7.14 (m, 3H), 4.73 (s, 4H), 4.15 (t, 2H, J = 7.6 Hz), 1.68–1.63(m, 2H), 1.46–1.38(m, 2H), 0.95 (t, 3H, J = 7.4 Hz). ^{13}C NMR (100 MHz, $CDCl_3$, δ): 164.5, 163.9, 157.3, 153.6, 149.6, 136.8, 131.9, 131.1, 130.3, 130.1, 126.7, 125.9, 123.4, 122.5, 122.3, 117.6, 116.7, 59.9, 40.0, 30.2, 20.4, 13.8. MS (FAB): $[M+H]^+$ calcd for $C_{28}H_{27}N_4O_2$, 451.2; found 451.3.

Preparation of 2. Under nitrogen, a solution of **3** (0.3 g, 0.76 mmol) and 3-aminopropyl-triethoxysilane (0.3 g, 1.36 mmol) in EtOH (50 mL) was refluxed for 24 h, the mixture was evaporated by rotary evaporation and the crude product was purified by column chromatography (silica, MC/EtOH 20:1) to give 0.37 g of **1** (82% yield). ^{1}H NMR (300

MHz, $CDCl_3$, δ): 8.87 (d, 1H, J = 8.5 Hz), 8.60–8.56 (m, 3H), 8.35 (d, 1H, J = 8.2 Hz), 7.71 (t, 1H, J = 8.5 Hz), 7.58 (t, 2H, J = 7.6 Hz), 7.34 (d, 2H, J = 7.8 Hz), 7.19–7.13 (m, 3H), 4.73 (s, 4H), 4.12 (t, 2H, J = 7.6 Hz), 3.79 (q, 6H, 7.0 Hz), 1.84–1.78(m, 2H), 1.19 (t, 9H, J = 7.0 Hz), 0.73 (t, 2H, J = 8.5 Hz). ^{13}C NMR (100 MHz, $CDCl_3$, δ): 164.4, 163.9, 157.3, 153.5, 149.5, 136.7, 131.9, 131.1, 130.2, 130.1, 126.7, 125.9, 123.4, 122.5, 122.3, 117.7, 116.7, 59.9, 58.4, 42.7, 21.5, 18.3, 7.97. MS (FAB): $[M+H]^+$ calcd for $C_{33}H_{39}N_4O_5Si$, 599.3; found 599.4.

Preparation of Mesoporous Silica. Mesoporous silica was synthesized starting from the preparation of a hydrochloric acid solution of P-123 [(poly(ethylene oxide)-poly(propylene oxide)-poly(ethylene oxide) triblock copolymer)]. Tetraethyl orthosilicate (TEOS) was then added and the mixture was stirred at 40 °C for 20 h. The molar composition was 1 : 5.9 : 193 : 0.017 TEOS : HCl : H_2O : P-123. The solid was aged at 65 °C for 1 day and was then filtered, washed and dried at 90 °C. To cleave the template to generate mesopores, 1.0 g of as-synthesized SBA-15 was mixed with 100 mL of 60 wt% H_2SO_4 solution and refluxed at 95 °C for 1 day. The product was recovered by washing with water and dried at 90 °C. To generate mesopores, the acid-treated sample was heated to 200 ^oC in air. To remove cationic surfactants from the resulting dried fiber-like flocculates and particles, the sample was calcined in a box furnace in air at 500 °C for 5 h, with a ramp rate of 1 °C/min.

Immobilization of Receptor 2 onto Mesoporous Silica. Compound **2** (100 mg) was dissolved in toluene (10 mL). The mesoporous silica (100 mg) was added as a solid. The suspension of silica was stirred under reflux conditions for 24 h in toluene. Then, the collected solid was washed copiously with toluene (50 mL) to rinse away any surplus **2** and dried under vacuum.

The **MSIND** has a BET (Brunauer–Emmett–Teller) surface area of 685.52 m^2/g and a pore volume of 0.28 cm^3/g (the mesoporous silica has a BET surface area of 1120.72 m^2/g and a pore volume of 0.50 cm^3/g). The mesoporous silica and the **MSIND** have BJH

(Barrett–Joyner–Halenda) pore diameters of 8.1 and 7.2 nm, respectively (Fig. S9). The decreased surface area and pore diameter in **MSIND** are attributable to the attachment of the receptor **2** to the mesoporous silica. Furthermore, the **MSIND** consists of only 18 wt% of **2**, as was determined from the results of TGA measurements (Fig.S10). For the mesoporous silica, IR peaks appear at 3480, 1850 and 1084 cm^{-1}, while for **MSIND** (Fig. S11), the peaks appear at 3475, 2979, 2935, 1685, 1650, 1578, 1525, 1435, 1446, 1408 and 1350 cm^{-1}. These new peaks originate from the receptor **2**, providing solid evidence that **2** is indeed attached to the surface of the mesoporous silica.

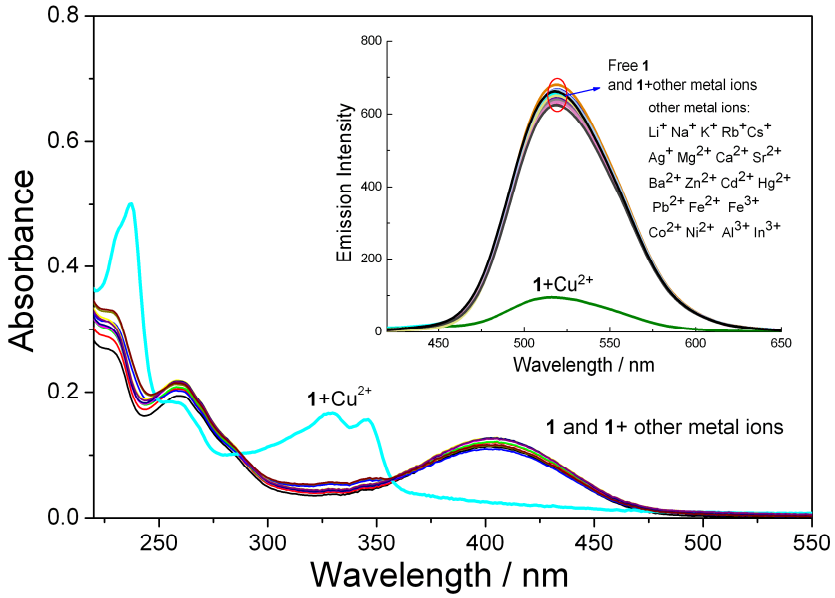

Figure S1. UV-Vis spectra and fluorescence spectra (λ_{ex} = 380 nm) (inset) of **1** (10 μM) and **1** in the presence of various metal ions anions perchlorate salts (10 equiv.) in HEPES buffer solution (0.02 M, pH = 7.4).

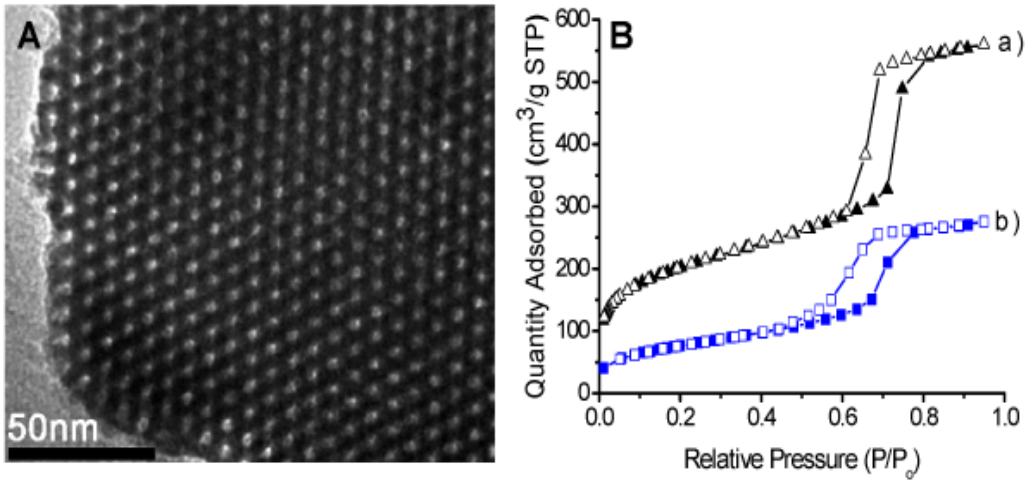

Figure S2. (A) TEM image of **MSIND**. (B) The nitrogen adsorption-desorption isotherms of (a) mesoporous silica and (b) **MSIND**.

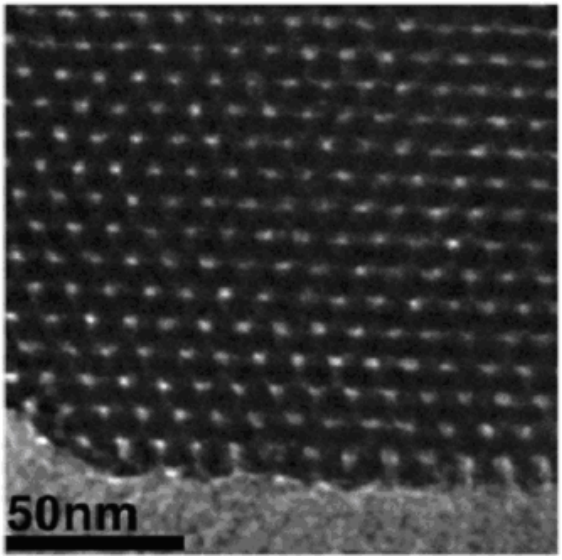

Figure S3. TEM image of mesoporous silica after calcination at 600 ^{o}C.

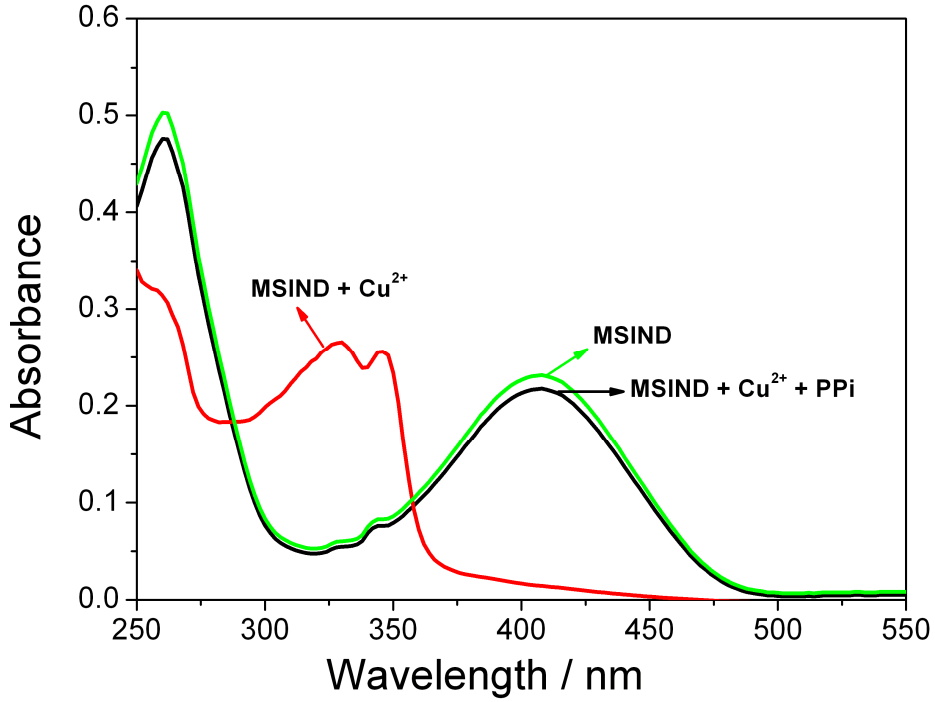

Figure S4. UV-vis spectra of (a) **MSIND** (10 μM) in the presence of (b) Cu^{2+} (10 μM) and (c) PPi (10 equiv.) in aqueous solution (pH 7.4).

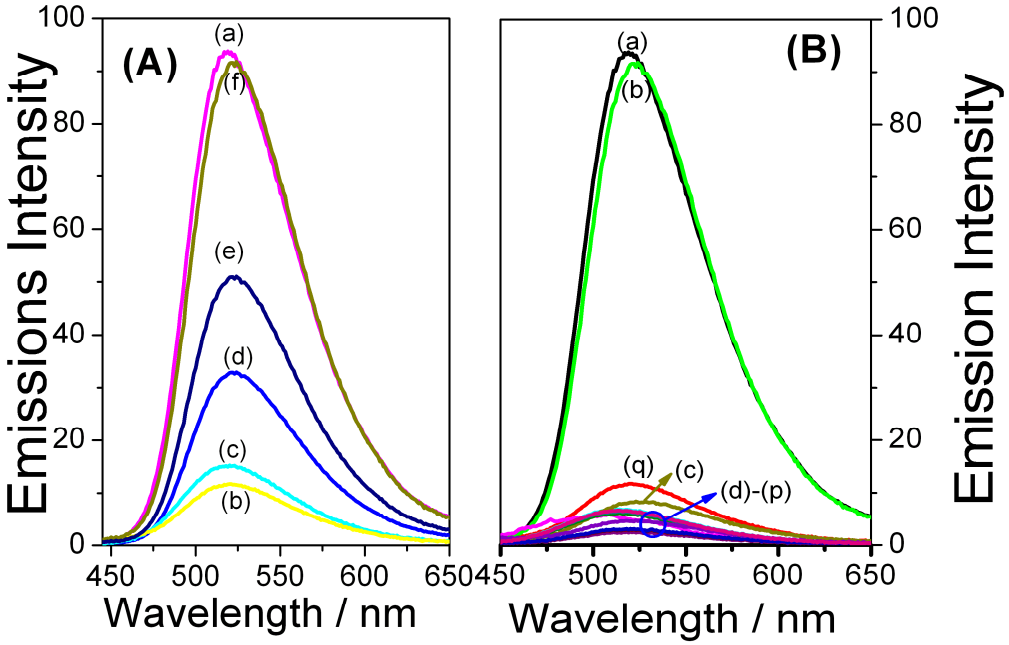

Figure S5. (A) Fluorescence spectra of (a) **MSIND** (10 μM) in the presence of (b) Cu^{2+} (10 μM) and (c-f) PPi (2, 5, 10, and 20 equiv). (B) Fluorescence spectra of (a) **MSIND** (10 μM) of 20 equiv. of (b) PPi (c) F^-, (d) Cl^-, (e) Br^-, (f) I^-, (g) OH^-, (h) CN^-, (i) SCN^-, (j) NO_3^-, (k) ClO_4^-, (l) SO_4^{2-}, (m) HCO_3^-, (n) CO_3^{2-}, (o) HSO_4^-, and (p) HPO_4^{2-} in the presence of (q) Cu^{2+} (10 μM).

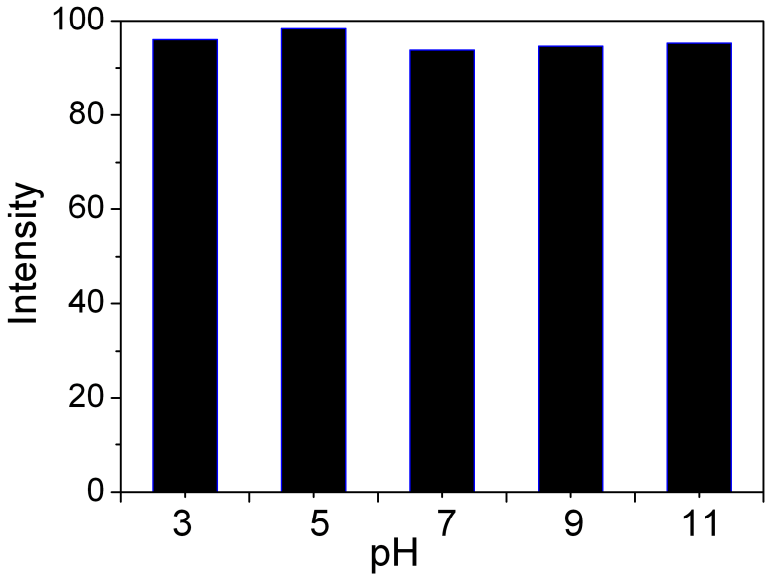

Figure S6. Fluorescence intensities of **MSIND-Cu** (10 μM) upon the addition of PPi (100 μM) at different pH values.

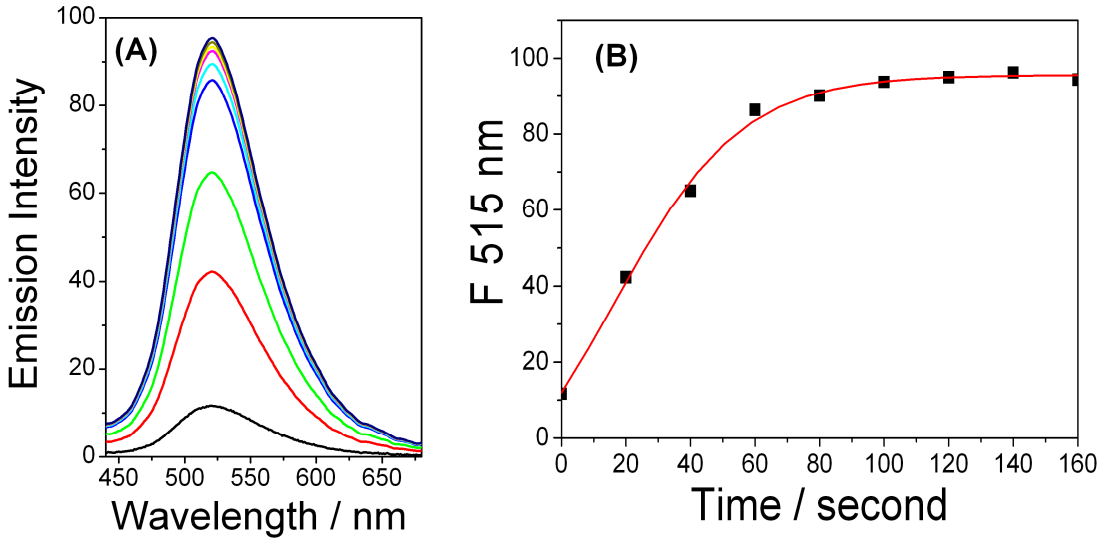

Figure S7. Time dependent fluorescence spectra of **MSIND-Cu** (10 μM) upon the addition of PPi (100 μM) in aqueous solution at pH 7.4 (A); and the fluorescence intensity at 515 nm as a function of time (B).

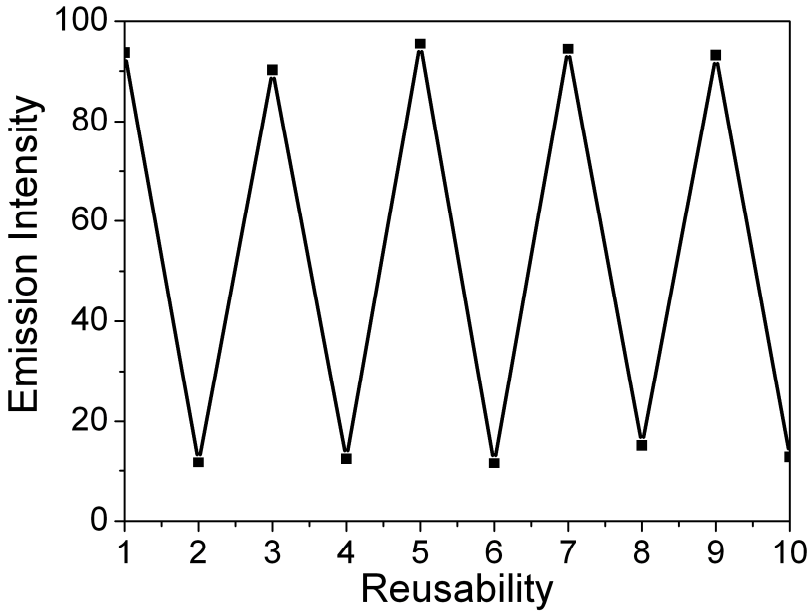

Figure S8. Plot for the emission of **MSIND-Cu** (10 μM**)** by alternated dipping in 10 μM aqueous solution of PPi ("ON") and 10 μM Cu^{2+} ("OFF"). The cyclic index is the number of alternating dipping/rinsing cycles, with the vertical axis showing the fluoresence for the **MSIND** at 515 nm.

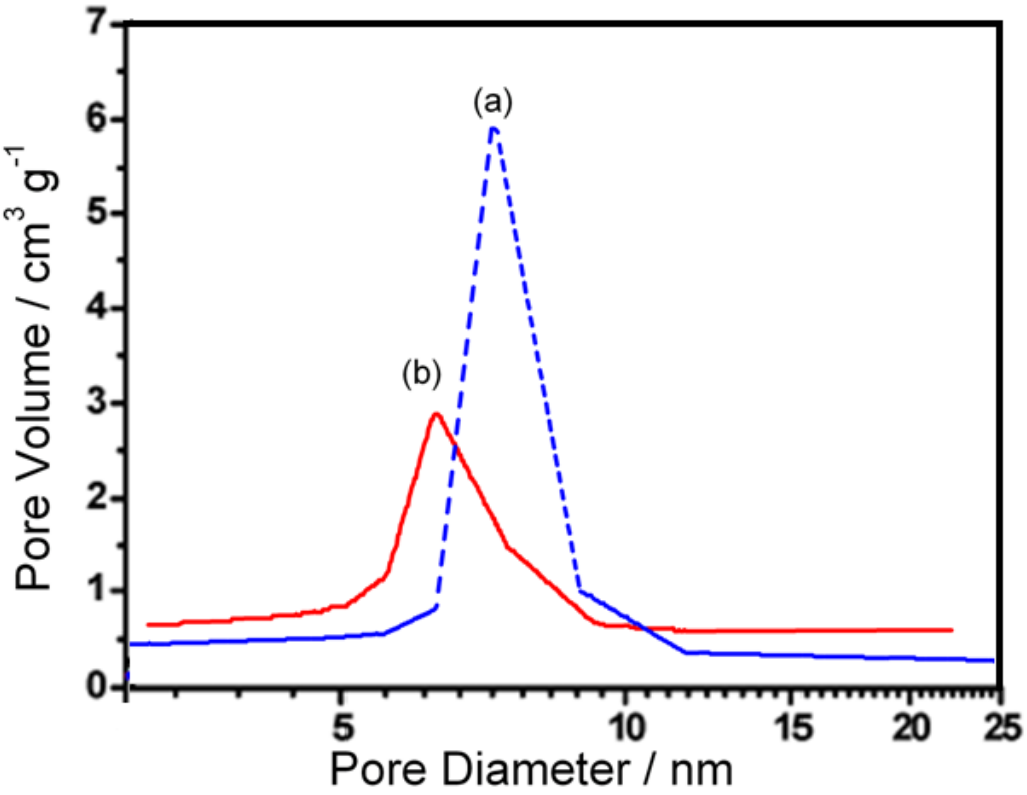

Figure S9. Barrett-Joyner-Halenda(BJH) pore diameters of (a) mesoporous silica and (b) **MSIND**.

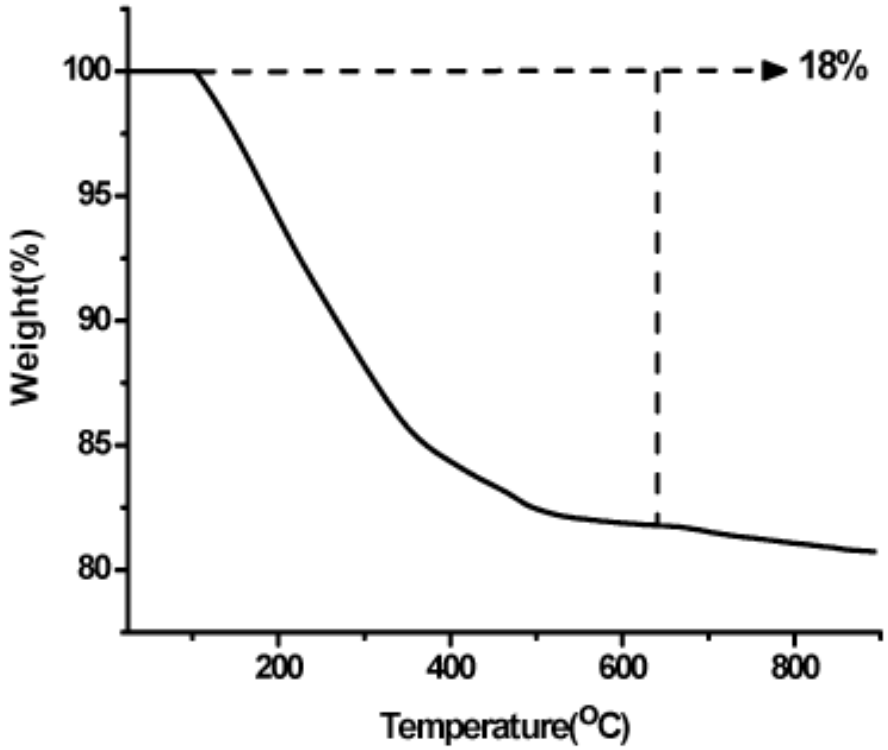

Figure S10. Thermogravimetric analysis data of **MSIND**.

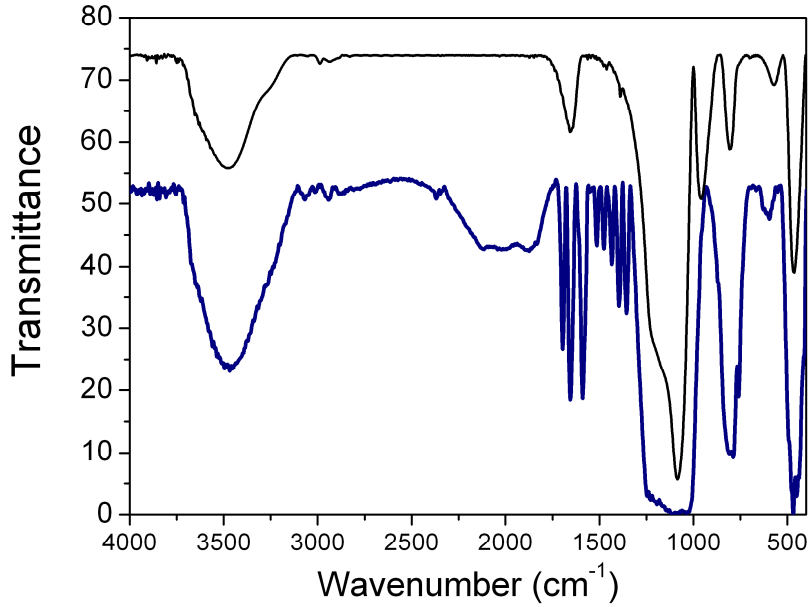

Figure S11. FT-IR spectra of (a) mesoporous silica (SBA-15) and (b) **MSIND**.

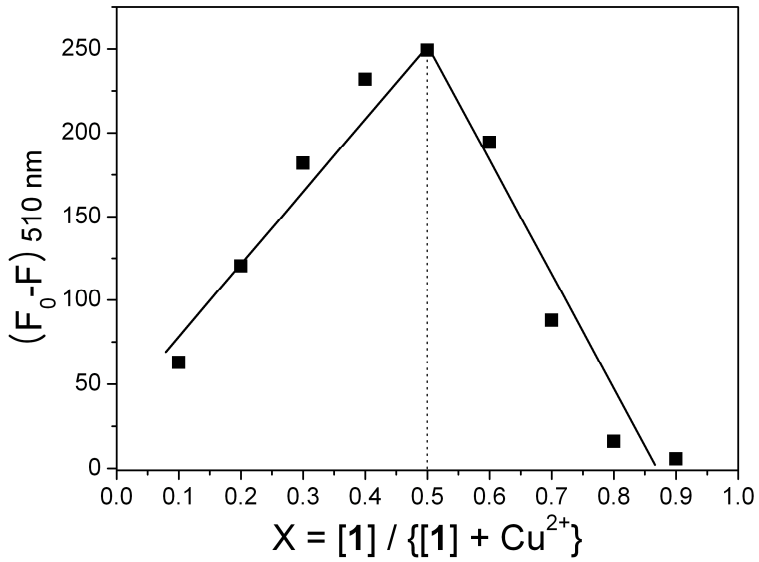

Figure S12. Job's plot showing the 1:1 binding of **1** to Cu^{2+} ions.

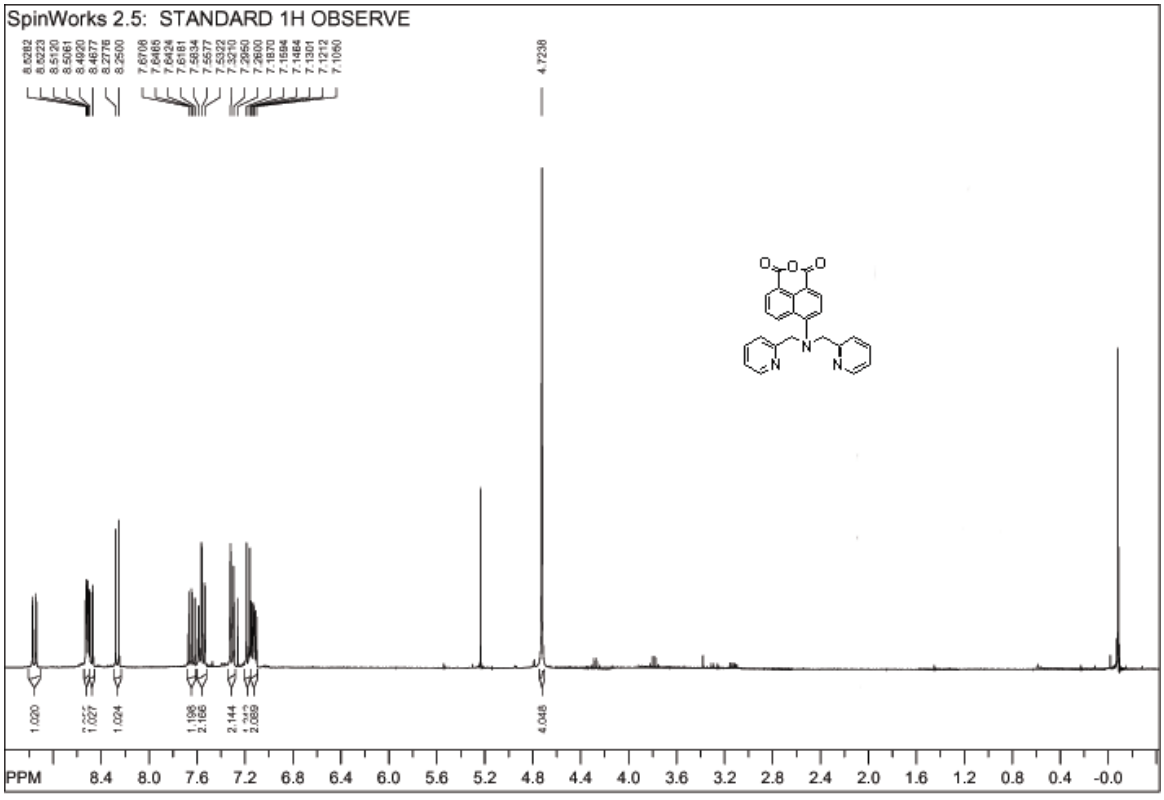

Figure S13. ^1H NMR spectrum of **3** recorded in $CDCl_3$.

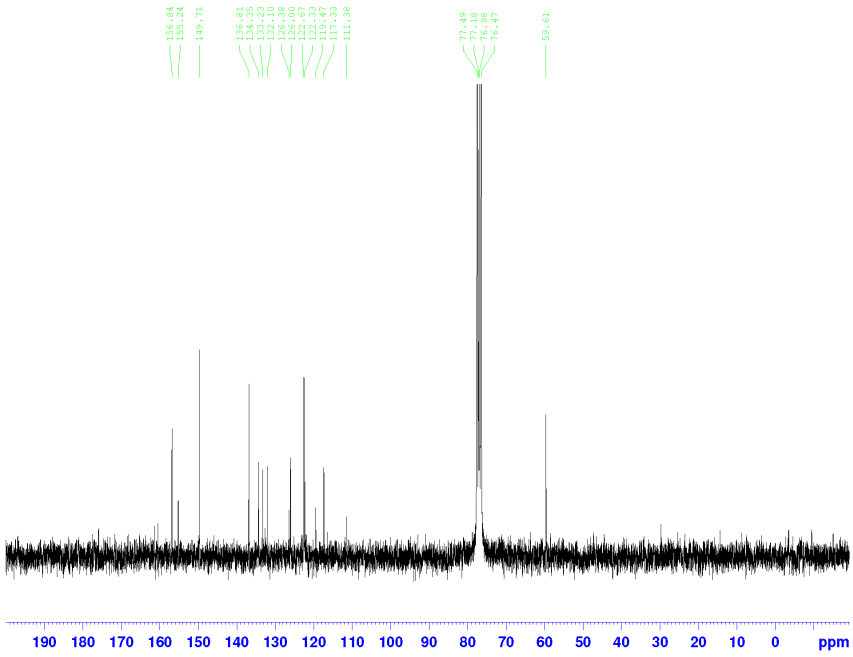

Figure S14. ^{13}C NMR spectrum of **3** recorded in $CDCl_3$.

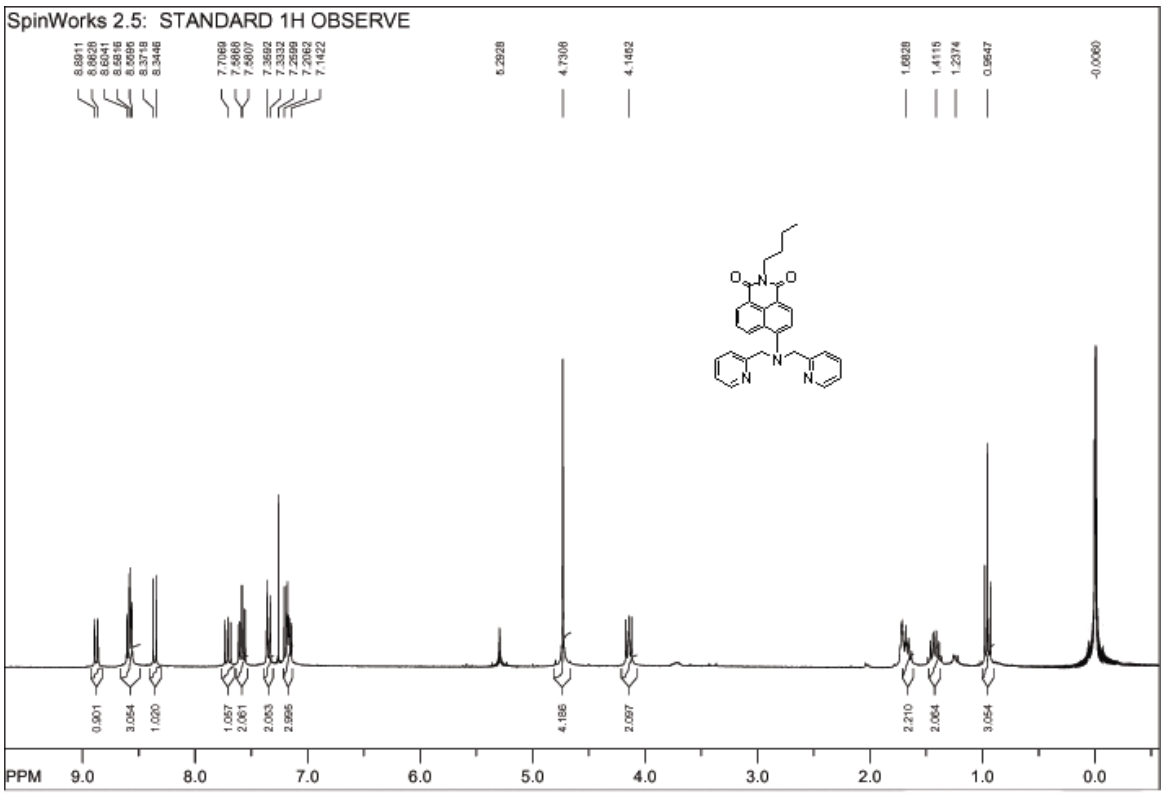

Figure S15. ^{1}H NMR spectrum of **1** recorded in $CDCl_3$.

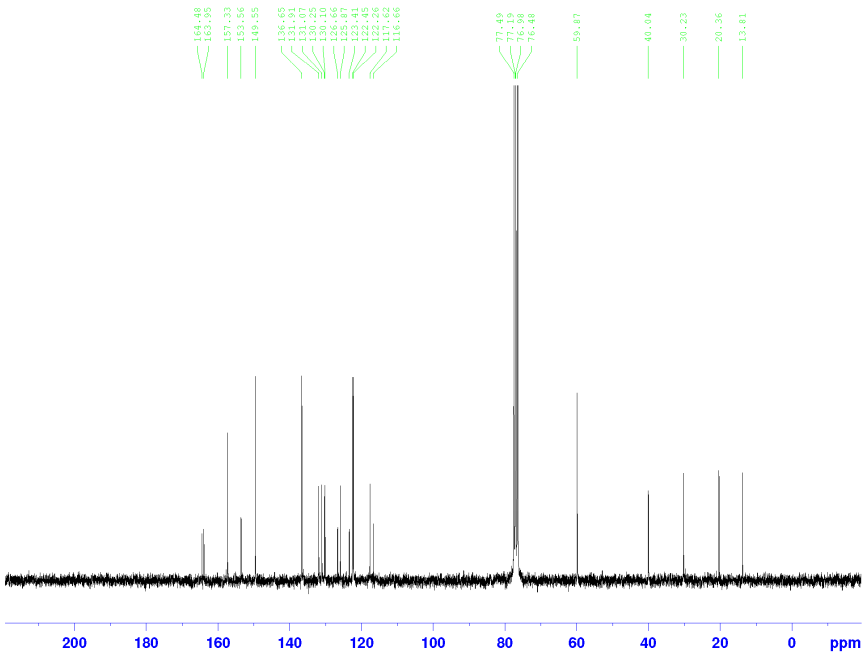

Figure S16. ^{13}C NMR spectrum of **1** recorded in $CDCl_3$.

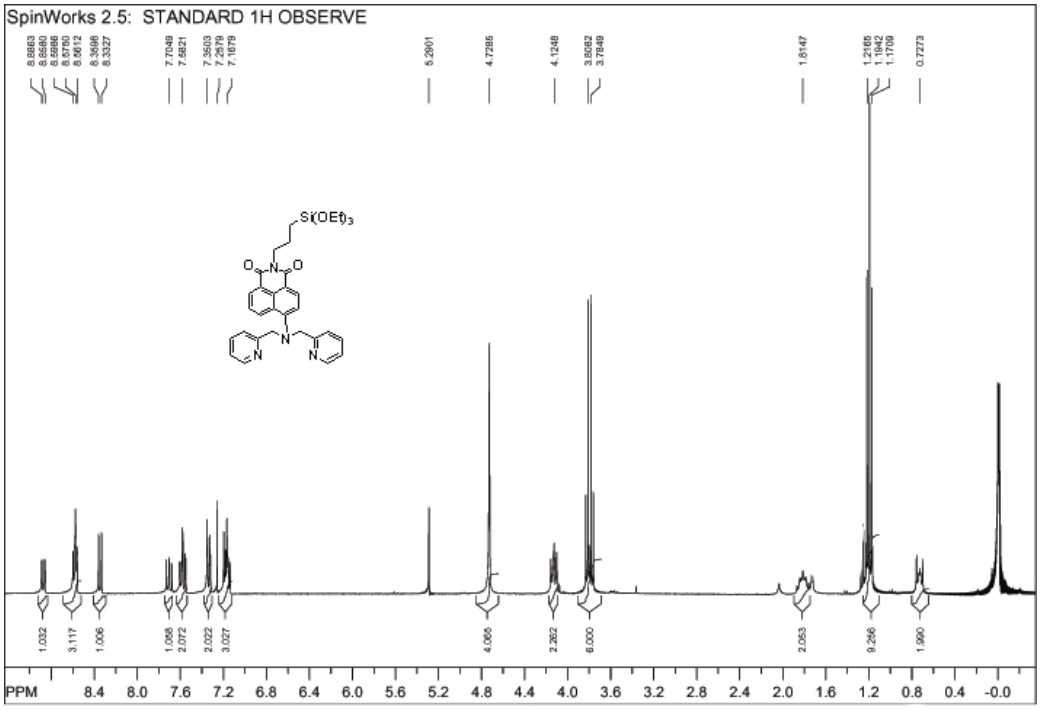

Figure S17. ^{1}H NMR spectrum of **2** recorded in $CDCl_3$.

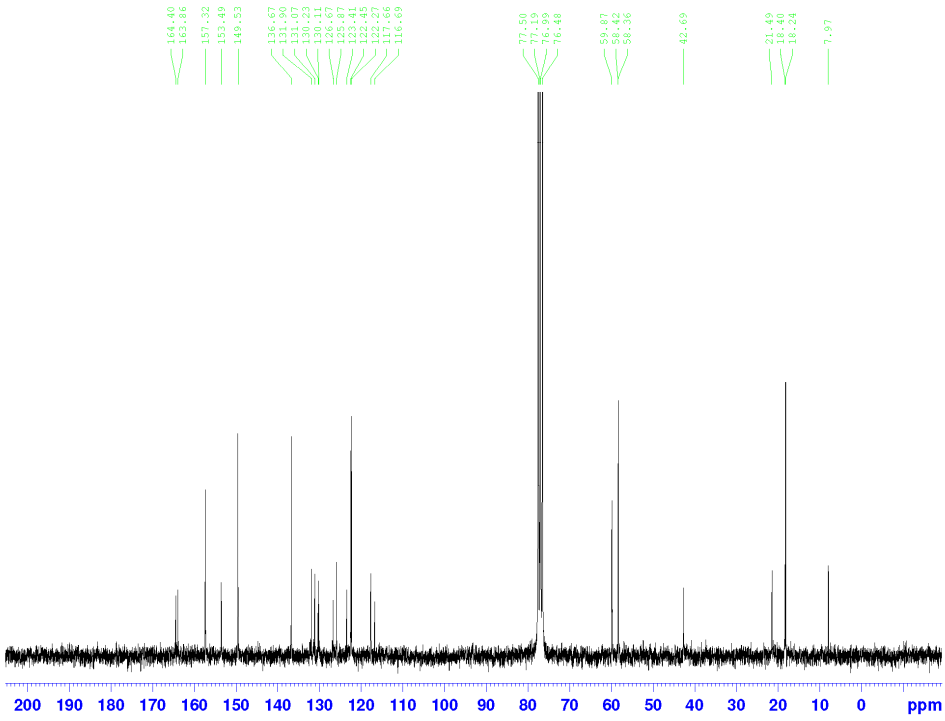

Figure S18. ^{13}C NMR spectrum of **2** recorded in $CDCl_3$.

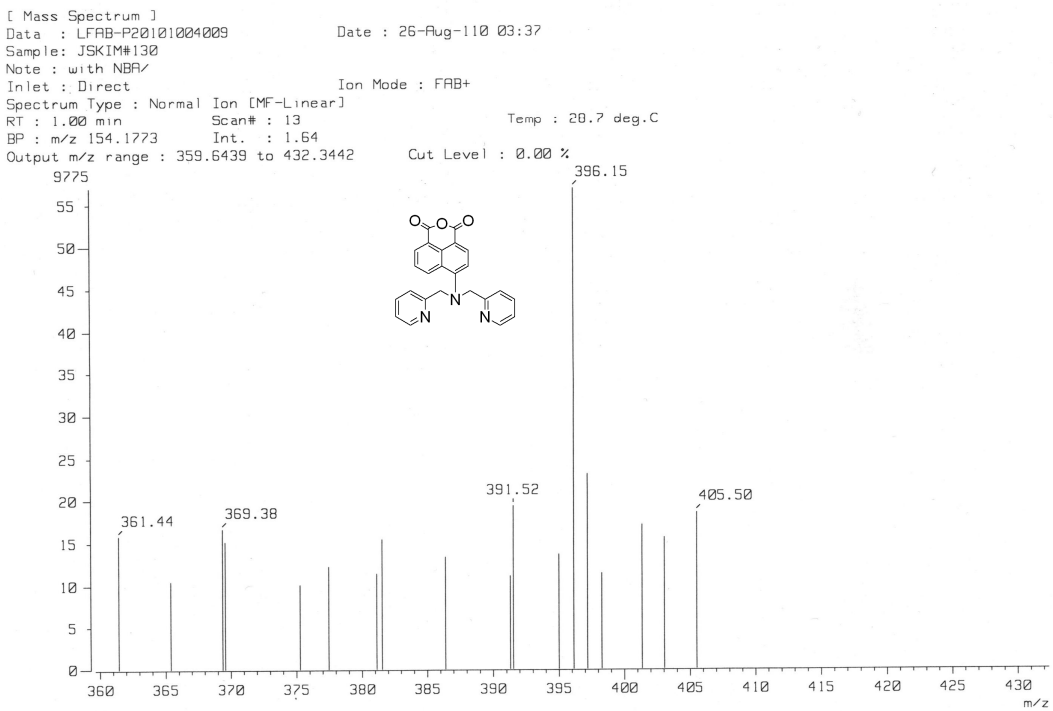

Figure S19. FAB-MS of **3**.

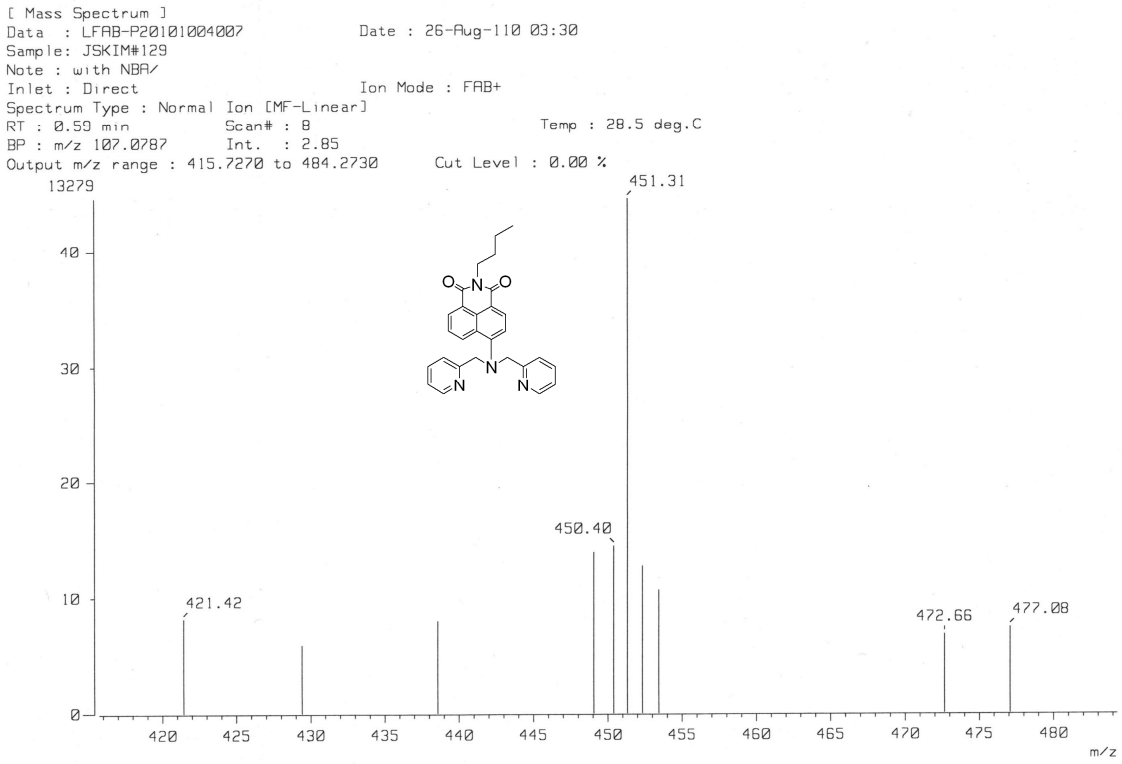

Figure S20. FAB-MS of **1**.

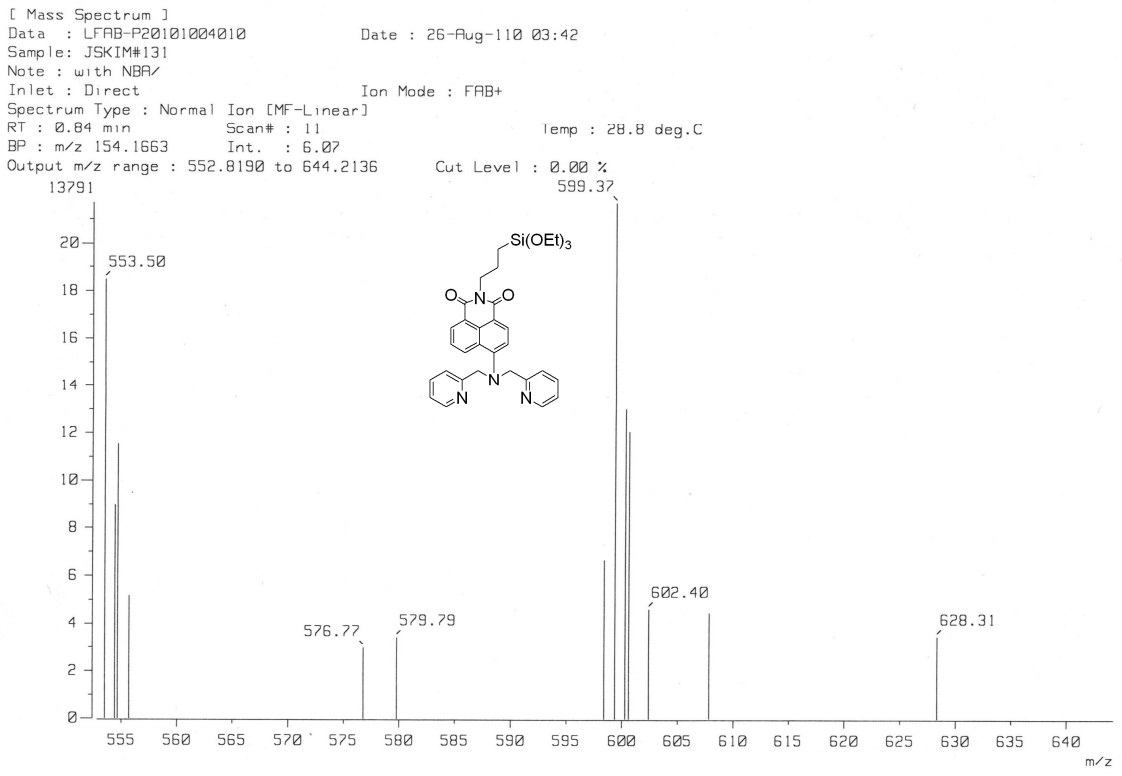

Figure S21. FAB-MS of **2**.

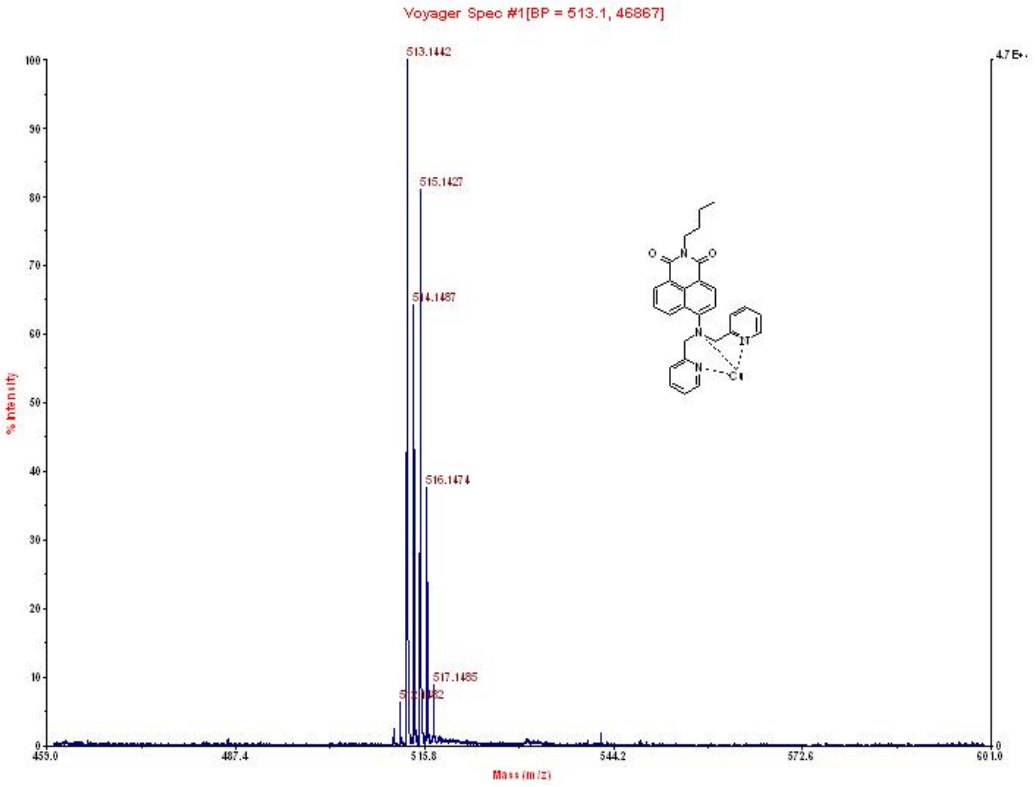

Figure S22. FAB-MS of **1-Cu**.

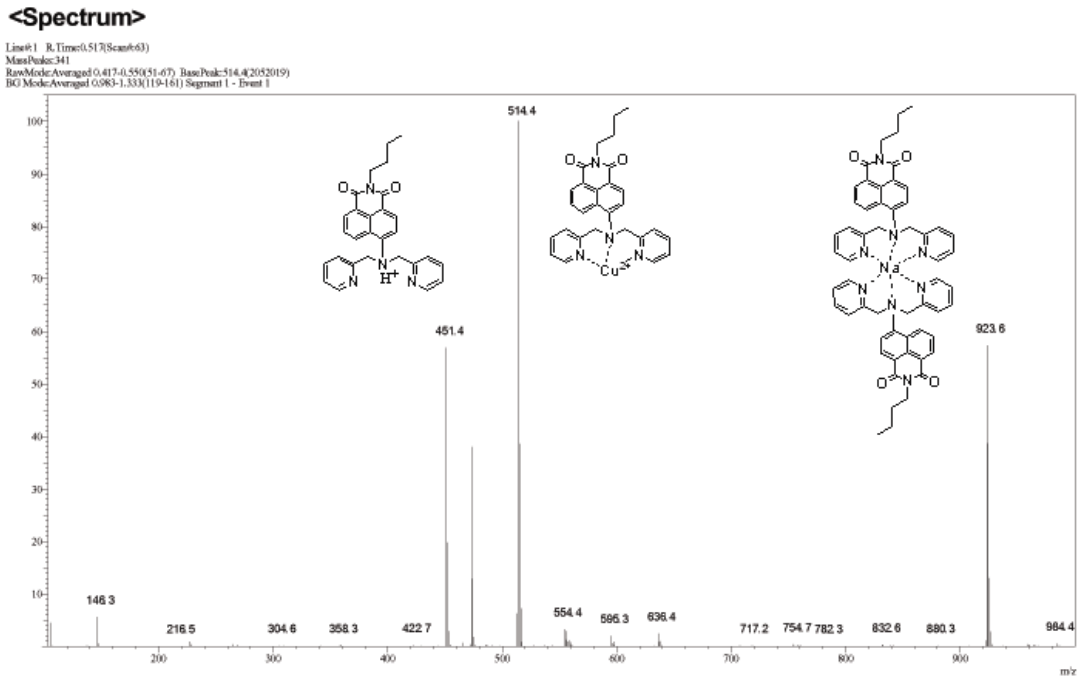

Figure S23. ESI-MS of **1-Cu** upon addition of $Na_4P_2O_7$ (sodium pyrophosphate) (5 equiv.).

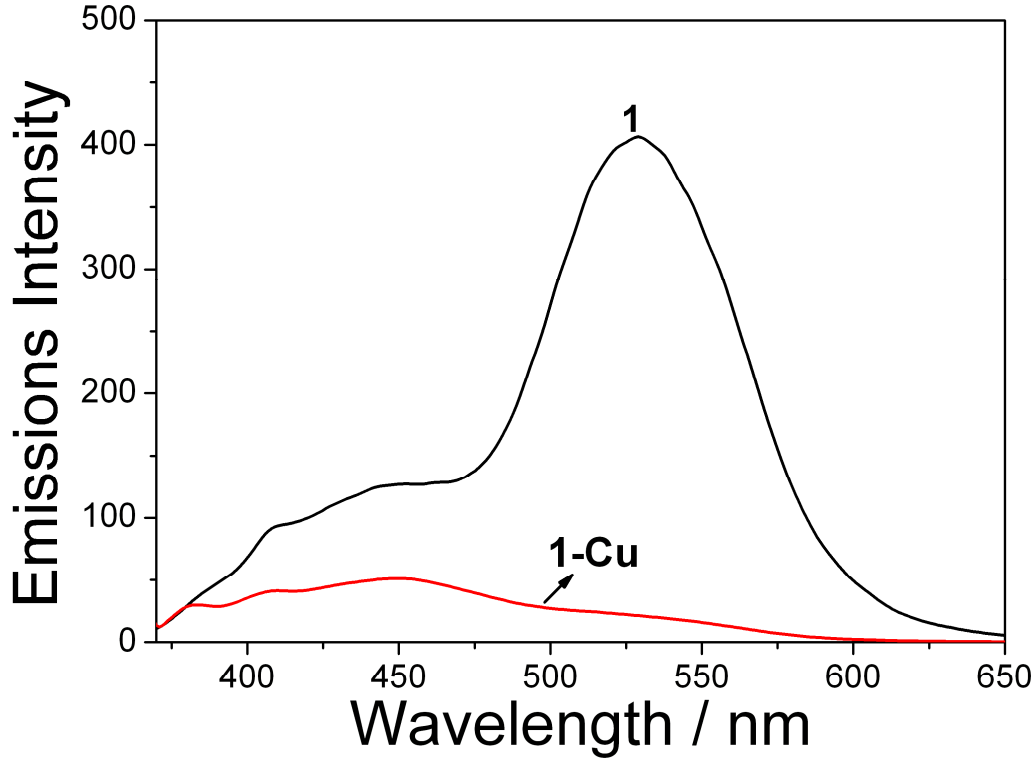

Figure S24. Fluorescence spectra (λ_{ex} = 358 nm) of **1** (10 μM) and **1-Cu** (10 μM) in HEPES buffer solution (0.02 M, pH = 7.4). The fluorescence quantum yields (Φ) of **1** and **1-Cu** were 0.17 and 0.02, respectively (quinoline sulfate in 0.1 N H_2SO_4 used as the standard for quantum yield measurements; Φ = 0.54).